Boggs, J. M., & Moscarello, M. A. (1978) *Biochemistry 17*, 5734.
Boggs, J. M., Clement, I. R., & Moscarello, M. A. (1980) *Biochim. Biophys. Acta 601*, 134.
Chapman, D., Cornell, B. A., Eliasz, A. W., & Perry, A. (1977) *J. Mol. Biol. 113*, 517.
Chen, S. C., & Sturtevant, J. M. (1981) *Biochemistry 20*, 713.
Cheng, W. H. (1980) *Biochim. Biophys. Acta 600*, 358.
Chowdry, B. Z., Lipka, G., Hajda, J., & Sturtevant, J. M. (1984) *Biochemistry 23*, 2044.
Davis, J. H. (1983) *Biochim. Biophys. Acta 737*, 117.
Davis, J. H., Clare, D. M., Hodges, R. S., & Bloom, M. (1983) *Biochemistry 22*, 5298.
Davis, P. J., & Keough, K. M. W. (1983) *Biochemistry 22*, 6334.
Eigenberg, K. E., Croasmun, W. R., & Chan, S. I. (1982) *Biochim. Biophys. Acta 679*, 353.
Flory, P. J. (1942) *J. Chem. Phys. 10*, 51.
Gomez-Fernandez, J. C., Goni, F. M., Bach, D., Restall, C. J., & Chapman, D. (1980) *Biochim. Biophys. Acta 598*, 502.
Guggenheim, E. A. (1952) *Mixtures*, Clarendon Press, Oxford.
Heyn, M. P., Blume, A., Rehorek, M., & Dencher, N. A. (1981) *Biochemistry 20*, 7109.
Hildebrand, J. H., & Scott, R. L. (1950) *The Solubility of Nonelectrolytes*, Reinhold, New York.
Hinz, H.-J., & Sturtevant, J. M. (1972) *J. Biol. Chem. 247*, 6071.
Huschilt, J. C. (1984) M.S. Thesis, University of Guelph, Guelph, Ontario, Canada.
Huschilt, J. C., Hodges, R. S., & Davis, J. H. (1985) *Biochemistry 24*, 1377–1386.
Jahnig, F. (1979) *J. Chem. Phys. 70*, 3279.
Keough, K. M. W., & Davis, P. J. (1979) *Biochemistry 18*, 1453.
Lee, A. G. (1977) *Biochim. Biophys. Acta 472*, 285.
Lee, A. G. (1978) *Biochim. Biophys. Acta 507*, 433.
Mabrey, S., & Sturtevant, J. M. (1976) *Proc. Natl. Acad. Sci. U.S.A. 73*, 3862.
Mabrey, S., & Sturtevant, J. M. (1979) *Methods Membr. Biol. 9*, 237.
Mabrey, S., Mateo, P. L., & Sturtevant, J. M. (1978) *Biochemistry 17*, 2464.
Marsh, D., Watts, A., & Knowles, P. F. (1977) *Biochim. Biophys. Acta 465*, 500.
Masón, J. T., Huang, C. H., & Biltonen, R. L. (1983) *Biochemistry 22*, 2013.
Mouritsen, O. G., & Bloom, M. (1984) *Biophys. J. 46*, 141.
O'Leary, T. J. (1983) *Biochim. Biophys. Acta 731*, 47.
Rowe, E. S. (1983) *Biochemistry 22*, 3299.
Ruppel, D., Kapitza, H. G., Galla, H. J., Sixl, F., & Sackmann, E. (1982) *Biochim. Biophys. Acta 692*, 1.
Semin, B. K., Saraste, M., & Wikstrom, M. (1984) *Biochim. Biophys. Acta 769*, 15.
Silvius, J. R., & Gagné, J. (1984a) *Biochemistry 23*, 3232.
Silvius, J. R., & Gagné, J. (1984b) *Biochemistry 23*, 3241.
Spink, C. H., Muller, K., & Sturtevant, J. M. (1982) *Biochemistry 21*, 6598.
Sturtevant, J. M. (1982) *Proc. Natl. Acad. Sci. U.S.A. 79*, 3963.
Swalin, R. A. (1972) *Thermodynamics of Solids*, Wiley, New York.
Tinker, D. O., & Low, R. (1982) *Can. J. Biochem. 60*, 538.
Vigo, C., Grossman, S. H., & Drost-Hansen, W. (1984) *Biochim. Biophys. Acta 774*, 221.

Incorporation and Translocation of Aminophospholipids in Human Erythrocytes†

David L. Daleke and Wray H. Huestis*
Department of Chemistry, Stanford University, Stanford, California 94305
Received December 21, 1984; Revised Manuscript Received April 25, 1985

ABSTRACT: Cell morphology changes are used to examine the interaction of exogenous phosphatidylserine and phosphatidylethanolamine with human erythrocytes. Short-chain saturated lipids transfer from liposomes to cells, inducing shape changes that are indicative of their incorporation into, and in some cases translocation across, the cell membrane bilayer. Dioleoylphosphatidylserine and low concentrations of dilauroyl- and dimyristoylphosphatidylserine induce stomatocytosis. At higher concentrations, dilauroylphosphatidylserine and dimyristoylphosphatidylserine induce a biphasic shape change: the cells crenate initially but rapidly revert to a discocytic and eventually stomatocytic shape. The extent of these shape changes is dose dependent and increases with increasing hydrophilicity of the phospholipid. Cells treated with dilauroylphosphatidylethanolamine and bovine brain lysophosphatidylserine exhibit a similar biphasic shape change but revert to discocytes rather than stomatocytes. These shape changes are not a result of vesicle–cell fusion nor can they be accounted for by cholesterol depletion. The reversion from crenated to stomatocytic forms is dependent on intracellular ATP and Mg^{2+} concentrations and the state of protein sulfhydryl groups. The present results are consistent with the existence of a Mg^{2+}- and ATP-dependent protein in erythrocytes that selectively translocates aminophospholipids to the membrane inner monolayer engendering aminophospholipid asymmetry.

A variety of methods have been developed for examining the asymmetric distribution of lipids across the erythrocyte membrane bilayer and other lipid membrane bilayer systems [for recent reviews, see Schwartz et al. (1985), Van Deenen (1981), Etemadi (1980), Op den Kamp (1979), and Roelofsen & Zwaal (1976)]. These techniques have established the asymmetric distribution of erythrocyte membrane lipids;

† This work was supported by a grant from the National Institutes of Health (HL 23787).

0006-2960/85/0424-5406$01.50/0

choline phospholipids, such as phosphatidylcholine (PC)[1] and sphingomyelin (SM), are found mostly in the outer membrane leaflet, and aminophospholipids or negatively charged phospholipids, such as phosphatidylserine (PS), phosphatidylethanolamine (PE), and phosphatidylinositol, are found primarily in the inner leaflet.

Other studies have focused on determining the mechanism by which red cells maintain this asymmetric distribution of lipids. The problem has been approached by perturbing the cell with a reagent having a known effect and then reassessing the bilayer asymmetry (Haest & Deuticke, 1976; Haest et al., 1978), and by adding a spin-labeled or radiolabeled lipid to the cell and following its fate spectrometrically (Seigneuret & Devaux, 1984) or by reextraction (Mohandas et al., 1978, 1982; Bergmann et al., 1984b). The precise mechanism by which the cell maintains this asymmetric distribution of lipids, however, has yet to be established. Work so far has implicated the involvement of erythrocyte cytoskeletal proteins (Haest et al., 1978) and has demonstrated that certain PS analogues translocate and accumulate in the inner monolayer (Bergman et al., 1984b; Dressler et al., 1984) in an ATP-dependent process (Seigneuret & Devaux, 1984).

The present work addresses the mechanism of red cell lipid asymmetry maintenance by introducing short-chain saturated PS and PE into cells from sonicated vesicles. Cells exposed to most such vesicles crenate transiently and then revert to severely stomatocytic forms. These morphological transformations are consistent with foreign lipid uptake (Deuticke, 1968; Sheetz & Singer, 1974; Mohandas & Feo, 1975; Fuji et al., 1979; Ferrell et al., 1985), followed by selective translocation to the membrane inner monolayer. Such morphological changes are used in the present work to examine a range of biochemical parameters that influence membrane phospholipid asymmetry.

Experimental Procedures

Materials. Dilauroylphosphatidylethanolamine (DLPE), dimyristoylphosphatidylserine (DMPS), dioleoylphosphatidylserine (DOPS), and bovine brain phosphatidylserine (brain PS) were purchased from Avanti Polar Lipids, Inc. Bovine brain lysophosphatidylserine (lyso-PS), dilauroylphosphatidylcholine (DLPC), and dimyristoylphosphatidylcholine (DMPC) were obtained from Sigma Chemical Co. Cholesterol oleate (cholesteryl [1-^{14}C]oleate and cholesteryl [1,2,6,7-^{3}H(N)]oleate) and the scintillation cocktail Aquasol were purchased from New England Nuclear. [^{14}C]DOPS (1,2-dioleoyl-L-3-phosphatidyl-L-[U-^{14}C]serine) was obtained from Amersham Corp. The reagent 3,4-dihydroxy-2-methylpropiophenone (U-0521) was a kind gift of the Upjohn Co., Kalamazoo, MI. Bovine serum albumin (essentially fatty acid free), iodoacetamide, dithiothreitol, diamide, and the calcium chelator quin2/AM were also purchased from Sigma. The ionophore A23187 and a luciferin–luciferase mixture were obtained from Calbiochem-Behring Corp., San Diego, CA. All other chemicals were reagent grade. Dilauroylphosphatidylserine (DLPS) was synthesized enzymatically from DLPC and purified as described (Comfurius & Zwaal, 1977).

Cells. Human erythrocytes were obtained from adult volunteers by venipuncture and collection into EDTA. Erythrocytes were pelleted by centrifugation, washed 3 times with 4 volumes of 150 mM NaCl (NaCl) and once with 4 volumes of 138 mM NaCl, 5 mM KCl, 6.1 mM Na_2HPO_4, 1.4 mM NaH_2PO_4, and 5 mM glucose, pH 7.4 (NaCl/P_i), and used within 8 h.

Human platelets were obtained from adult volunteers who denied taking medication for the previous 14 days. Blood was collected by venipuncture into silicone-coated, acid–citrate-containing Vacutainer (B-D) tubes. Platelet-rich plasma was prepared by centrifugation at 150*g* for 15 min at room temperature, followed by a second centrifugation to remove residual leukocyte and erythrocyte contamination. The plasma was applied to a 2.5 × 18 cm Sepharose CL-2B column at 37 °C. Platelets were eluted at 37 °C with 137 mM NaCl, 2.7 mM KCl, 2 mM $MgCl_2$, 0.42 mM Na_2HPO_4, 5.6 mM glucose, and 5 mM HEPES, pH 7.4. Platelet fractions were pooled and allowed to rest at 37 °C for 1 h before use. Platelet concentration, as determined by hemocytometry, was 1.65 × 10^8 cells mL^{-1}.

Unless otherwise indicated, all incubations were conducted in NaCl/P_i at 37 °C, 50% hematocrit, in capped plastic tubes.

Vesicle Preparation. Unilamellar vesicles were prepared by sonicating a suspension of lipid (concentrations as noted) in NaCl/P_i under argon in a bath sonicator, at least 10 °C above the T_c of the particular lipid, until clear. In some experiments, lipid mixtures were prepared: DMPS (or DMPC) was cosonicated with [^{14}C]cholesteryl oleate (2.0 μCi, 53.1 mCi mmol^{-1}), DLPC (0.10 mM) was cosonicated with DLPS (0.10 mM), and DOPS (5 mM) was cosonicated with [^{14}C]DOPS (0.25 μCi, 60 mCi mmol^{-1}) and [^{3}H]cholesteryl oleate (1.25 μCi, 72 Ci mmol^{-1}).

Vesicle–Cell Incubations. Sonicated vesicles were incubated with cells at 50% hematocrit for the time intervals specified in the figure legends. In some experiments, cells were separated from exogenous vesicles by centrifugation, washed extensively with NaCl or NaCl/P_i, and incubated further in NaCl/P_i. For extended incubations (greater than 6 h), NaCl/P_i was supplemented with 10 mM inosine, 1 mM adenosine, 5 mM glucose, and antibiotics (100 μg mL^{-1} penicillin, 40 μg mL^{-1} neomycin) every 10–12 h.

Amino Acid Transporter Inhibition. (*A*) *Treatment with U-0521.* Because the reagent U-0521, an inhibitor of the red cell amino acid transporter (Floud & Fann, 1981), oxidizes rapidly upon sonication, it was added to cells as a 10-fold concentrate concurrently with a 0.56 mM sonicated DMPS solution to yield 1 mM U-0521 and 0.5 mM DMPS. Control cells were incubated with 1 mM U-0521 in the absence of DMPS.

(*B*) *Tryptophan + Leucine.* In other experiments, cells were incubated in 40 mM tryptophan, 40 mM leucine, and 115 mM NaCl, pH 7.4, with or without 0.5 mM DMPS.

Magnesium and Calcium Depletion. Cells were incubated at 20% hematocrit with 6.7 μM A23187 (added as a 400-fold concentrate in ethanol to a 37 °C suspension of cells, final [EtOH] = 0.4%) in NaCl/P_i ± 1 mM EDTA or EGTA for 10 min. Control cells were treated with ethanol in NaCl/P_i ± 1 mM EDTA or EGTA. The cells were washed once with 0.1% albumin in NaCl/P_i and once with NaCl/P_i prior to incubation with 0.5 mM DMPS vesicles. Cells were depleted of free intracellular calcium by chelation with quin2/AM

[1] Abbreviations: PC, phosphatidylcholine; SM, sphingomyelin; PS, phosphatidylserine; PE, phosphatidylethanolamine; DLPE, dilauroylphosphatidylethanolamine; DLPS, dilauroylphosphatidylserine; DMPS, dimyristoylphosphatidylserine; DOPS, dioleoylphosphatidylserine; brain PS, bovine brain phosphatidylserine; lyso-PS, bovine brain lysophosphatidylserine; DLPC, dilauroylphosphatidylcholine; DMPC, dimyristoylphosphatidylcholine; EDTA, ethylenediaminetetraacetic acid; HEPES, *N*-(2-hydroxyethyl)piperazine-*N*′-2-ethanesulfonic acid; EGTA, ethylene glycol bis(β-aminoethyl ether)-*N*,*N*,*N*′,*N*′-tetraacetic acid; Tris, tris(hydroxymethyl)aminomethane; MI, morphological index; DTNB, 5,5′-dithiobis(2-nitrobenzoic acid); TLC, thin-layer chromatography.

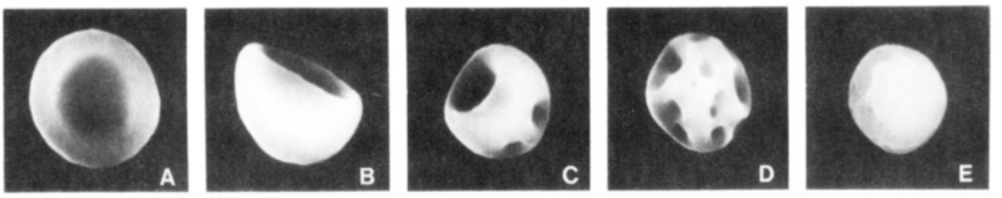

FIGURE 1: Scanning electron micrographs of erythrocytes at various stages of stomatocytosis: (A) stage 0 (discocyte); (B) stage −1; (C) stage −2; (D) stage −3; (E) stage −4. Magnification 2200×.

(Tsien, 1981). Quin2/AM (0.1 mM) was added to a 20% hematocrit suspension of cells, at 37 °C, as a 250-fold concentrate in ethanol. After incubation for 20 min, the cell suspension was diluted 4-fold and further incubated for 40 min. This treatment should result in 0.2 mM intracellular quin2 (Tsien et al., 1982). The cells were washed once with NaCl/P_i before treatment with 0.5 mM DMPS.

Magnesium Repletion. Cells were incubated with 1 mM EDTA in 100 mM KCl, 50 mM NaCl, 6.1 mM Na_2HPO_4, 1.4 mM NaH_2PO_4, and 5 mM glucose, pH 7.4 (KCl/P_i), ±5 μM A23187 as above. The cells were washed once with 0.1% albumin in KCl/P_i and twice with KCl/P_i. After incubation in KCl/P_i ± 0.5 mM DMPS, the cells were washed 4 times and then reincubated in KCl/P_i containing 1 mM $MgCl_2$, 1 μM EGTA, and 5 μM A23187.

ATP Depletion. (*A*) *Iodoacetamide and Inosine Treatment.* Erythrocytes were incubated with 6 mM iodoacetamide + 10 mM inosine in NaCl/P_i, 20% hematocrit, for 15 or 30 min to effect rapid ATP depletion (Lew, 1971). The cells were washed 3 times with NaCl/P_i prior to incubation with vesicles or NaCl/P_i.

(*B*) *Slow Metabolic Depletion.* Erythrocytes were incubated in 140 mM NaCl, 10 mM Tris, and 1 mM $MgSO_4$, pH 7.4, under humidified argon, without nutrients, for 13.5 h to metabolically deplete intracellular ATP (Nakao et al., 1960). Penicillin (100 μg mL^{-1}) and neomycin (40 μg mL^{-1}) were included to retard bacterial growth. The cells were washed once with NaCl/P_i and incubated with vesicles or NaCl/P_i.

ATP Repletion. After a 1-h incubation with vesicles or NaCl/P_i, cells were washed 3 times with NaCl/P_i and resuspended in NaCl/P_i supplemented with 10 mM inosine, 1 mM adenosine, 5 mM glucose, and antibiotics.

Diamide Treatment. Erythrocytes were incubated at 20% hematocrit for 1 h with 0.2, 1.0, or 5.0 mM diamide in NaCl/P_i. The cells were washed 4 times with NaCl/P_i before incubation with 0.5 mM DMPS. In other experiments, cells were first treated with 0.5 mM DMPS for 30 or 60 min, washed twice with NaCl/P_i, and treated with 5 mM diamide as above. Additionally, 5 mM diamide treated cells were incubated with 0.5 mM DMPS; aliquots were washed twice with NaCl/P_i at 30 and 60 min and incubated with 10 mM dithiothreitol in NaCl/P_i at 20% hematocrit. Control cells were treated with DMPS, washed twice with NaCl/P_i, and incubated with 10 mM dithiothreitol as above.

Assays. (*A*) *Morphology.* Erythrocytes were prepared for morphological indexing by fixing 5-μL aliquots of cell suspension for 10 min in 50 μL of a solution of 0.5% glutaraldehyde in 0.15 M NaCl. Platelets were fixed for 15 min with 1% glutaraldehyde in 0.15 M NaCl. Cells were viewed by light microscopy under bright field illumination and indexed on the basis of the grading scale of Fuji et al. (1979). Crenated cells (echinocytes) were given scores of +1 to +5 (Ferrell & Huestis, 1984), discocytes were given a score of 0, and cupped or invaginated cells (stomatocytes) were given scores of −1 to −4 (Figure 1). Platelet morphology was classified as discoid or spherical without filopodia (0), discoid with one or two filopodia (+1), or spherical with more than 2 filopodia (+2). The average score of a field of 100 erythrocytes or platelets was taken as the morphological index (MI).

Morphological indexing was normally performed on cell samples taken in nonrandom order. However, identical results (MI = ±0.2) were obtained when randomized, blind coded samples were reindexed.

Fixed cells were prepared for scanning electron microscopy by washing 4 times with distilled water, freeze-drying 2.5 μL of a 1% hematocrit suspension on a glass coverslip, and sputter coating with 18-nm gold–paladium before viewing.

(*B*) *Cholesterol and Phospholipids.* Samples were prepared for cholesterol and phospholipid analysis by extraction (Bligh & Dyer, 1959). Aliquots of cell suspension supernatant were added to 18 volumes of 2:1 methanol/chloroform, and the mixture was vortexed. Water (6 volumes) and chloroform (6 volumes) were added, the organic and aqueous phases were separated by centrifugation, and the reserved organic layer was evaporated by a nitrogen stream.

Cholesterol was assayed by a micro adaptation of the method of Zlatkis et al. (1953). Samples for lipid analysis were reconstituted with chloroform and spotted on silica gel HL plates (Analtech). After elution with 65:25:5 chloroform/methanol/formic acid, spots were visualized with iodine and scraped into tubes for phosphate analysis. Phospholipid phosphate was determined by the method of Bartlet (1959), after correction for silica background. The use of formic acid in the chromatographic solvent system decreases the tailing of PS found with acetic acid eluents, improving resolution of the four major classes of erythrocyte phospholipids (SM, PC, PS, and PE).

(*C*) *Scintillation Counting.* Samples were prepared for scintillation counting by bleaching aliquots overnight at 60 °C in 1 mL of 30% hydrogen peroxide + 0.1 mL of Aquasol to prevent foaming. After the samples were cooled, 10 mL of Aquasol was added, and vials were counted by using a Beckman LS-3150T scintillation counter.

(*D*) *ATP.* Frozen aliquots of cell suspension (equivalent to 10 μL of packed cells) were diluted to 3 mL with NaCl, boiled for 15 min, and centrifuged to clarity. The supernatant (diluted 1:10 or undiluted) was assayed for ATP by the luciferin–luciferase method (Kimmich et al., 1975).

(*E*) *Reduced Glutathione.* Aliquots of cell suspension (equivalent to 8 μL of packed cells) were lysed in 12.5 volumes of distilled water, proteins were precipitated with 0.21 M H_3PO_4, 6 mM EDTA, and 5.1 M NaCl, and samples were centrifuged to clarity. Supernatants were stored frozen and assayed for reduced glutathione by reaction with 5,5′-dithiobis(2-nitrobenzoic acid) (DTNB) (Beutler, 1975).

RESULTS

Stomatocyte Morphology. The stages of erythrocyte stomatocytosis are shown in Figure 1. Stage −1 stomatocytes are cup-shaped cells with one large concavity or are triconcave. As the cells become more stomatocytic, they develop small invaginations but retain one large concavity (stage −2). Al-

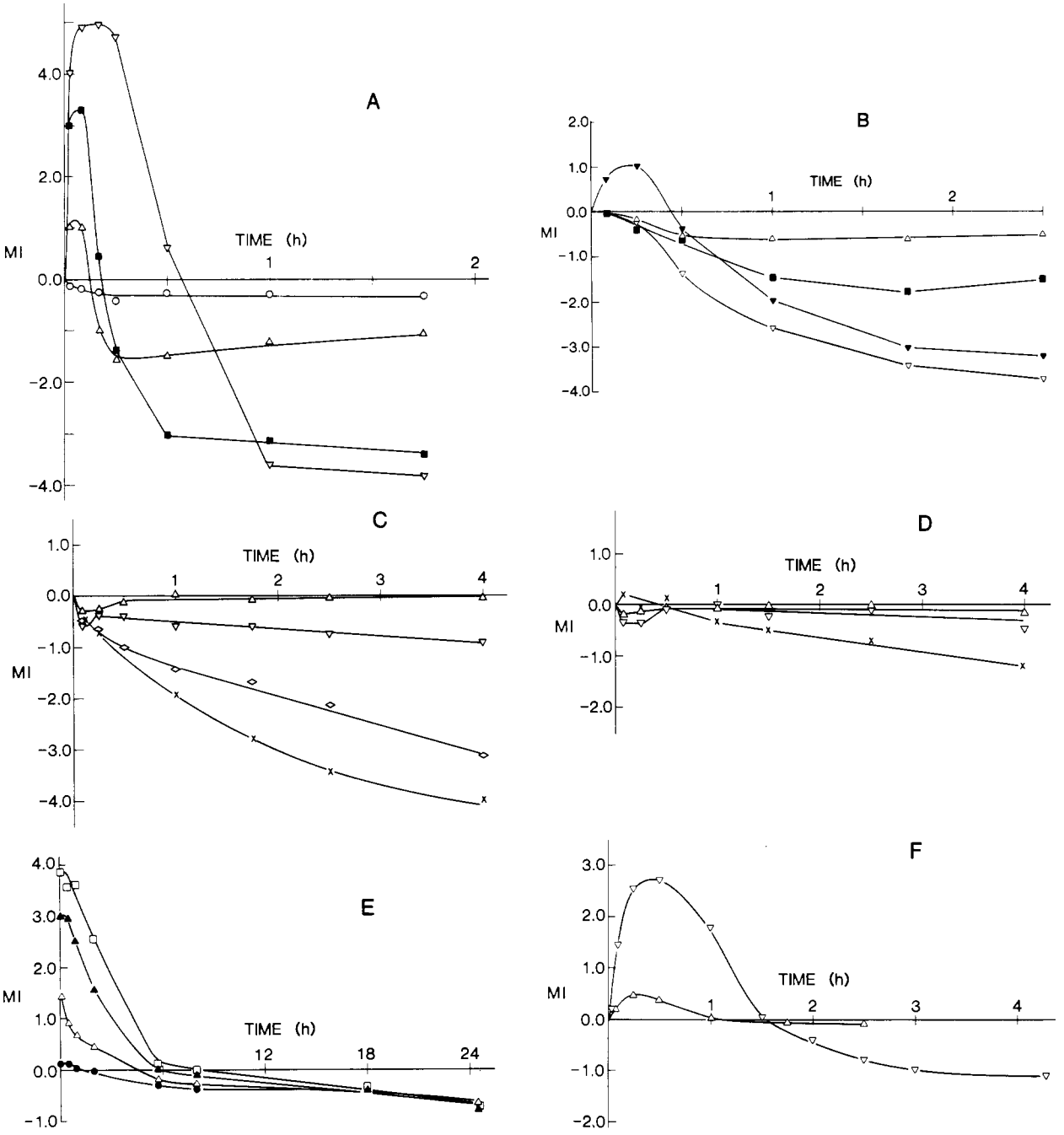

FIGURE 2: Time course of erythrocyte shape change (MI) during incubation with (A) DLPS, (B) DMPS, (C) DOPS, (D) brain PS, (E) lyso-PS, or (F) DLPE. Lipid concentrations (millimolar): 0.01 (○); 0.05 (●); 0.10 (△); 0.15 (▲); 0.20 (□); 0.25 (■); 1.0 (▽); 2.5 (▼); 5.0 (◇); 10.0 (×).

ternately, stage −2 cells may possess a ruffled concavity without acquiring invaginations. More severely stomatocytic cells become spherical, lose their large concavity, and acquire many smaller invaginations (stage −3). Endocytosis ensues, and stage −4 cells possess only a few residual invaginations or are smooth spheres containing endocytosed vesicles.

Phosphatidylserine-Induced Shape Changes. Erythrocytes incubated with DLPS vesicles underwent a complex shape transformation. As shown in Figure 2A, the cells became transiently echinocytic, then reverted to discocytes, and eventually became severely stomatocytic. The cells retained this stomatocytic shape even after extended (70–90 h) incubation.

The time course and extent of these morphological responses depended on the concentration and acyl chain composition of the vesicle lipid. Figure 2A–E shows the time course of erythrocyte shape changes induced by lyso-PS micelles and vesicles of DLPS, DMPS, DOPS, and brain PS at a variety of concentrations. DLPS above 0.1 mM and DMPS above 1 mM (Figure 2B) induced the biphasic discocyte to echinocyte to stomatocyte shape change. DOPS (0.1–10 mM, Figure 2C), brain PS (0.1–10 mM, Figure 2D), and lower concentrations of DLPS and DMPS (<0.1 and 1 mM, respectively) induced stomatocytosis directly, without initial crenation. Higher concentrations of DLPS and DMPS (1 and 10 mM, respectively) produced echinocytosis and subsequent stomatocytosis, accompanied by extensive hemolysis. Lyso-PS-treated cells also crenated rapidly but reverted to discocytes only very slowly (Figure 2E). Stomatocytosis was not extensive in such cells even after many hours of incubation.

Phosphatidylethanolamine-Induced Shape Changes. DLPE treatment induced cell morphology changes with the time

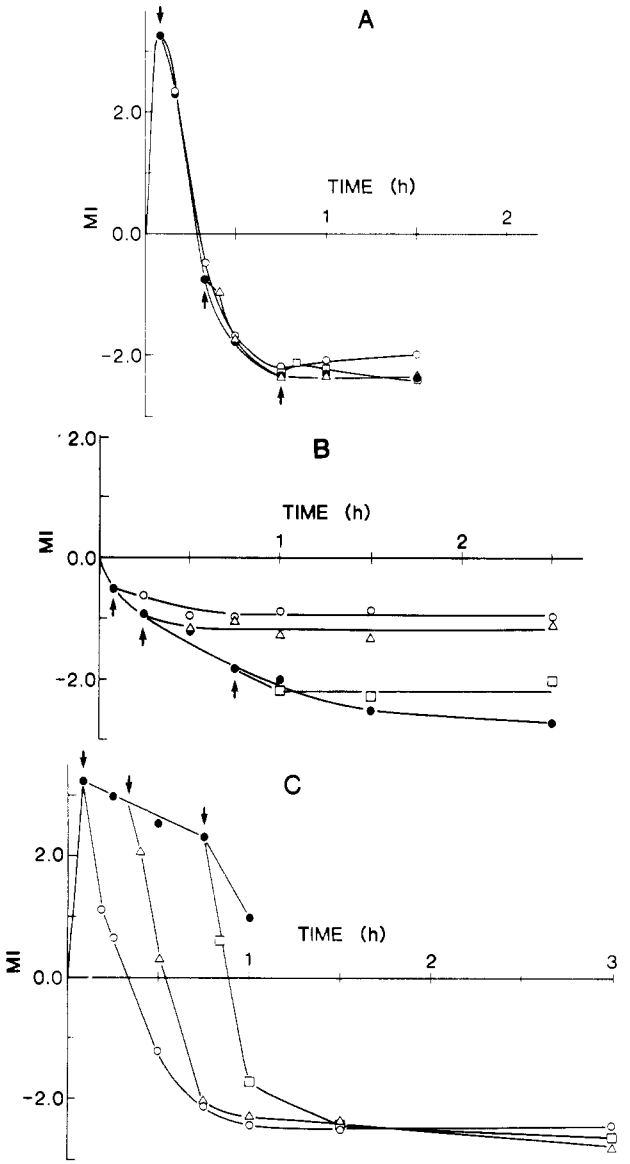

FIGURE 3: Effect of removing exogenous vesicle lipid on erythrocyte shape change from cells treated with (A) 1 mM DLPS, (B) 1 mM DMPS, and (C) 5 mM DMPS (●). Vesicles were removed by washing after 5 (○), 15 (△), or 45 (□) min of incubation, as indicated by arrows.

course and concentration dependence shown in Figure 2F. Cells exposed to 0.1 mM DLPE became transiently echinocytic, followed by a reversion to a discocytic or slightly stomatocytic shape. A higher concentration of DLPE (1 mM) produced a larger degree of both echinocytosis and stomatocytosis, though not as extreme as with DLPS at the same concentrations (Figure 2A,F, inverted triangles).

Effect of Removing Exogenous Lipid. After brief incubations, erythrocytes were washed free of exogenous lipid vesicles, and the ensuing shape changes were monitored. Cells were first incubated with DLPS (1 mM) or DMPS (1 and 5 mM), and after various time intervals (5, 15, or 45 min), the exogenous vesicles were removed by centrifugation and washing. As shown in Figure 3A, removal of exogenous DLPS had little effect on either the time course or the extent of shape change; 5 min of exposure sufficed to induce eventual severe stomatocytosis. In contrast, cells exposed to 1 mM DMPS stopped changing shape after being washed (Figure 3B). A higher concentration of DMPS (5 mM) produced rapid stomatocytosis after removal of exogenous lipid (Figure 3C).

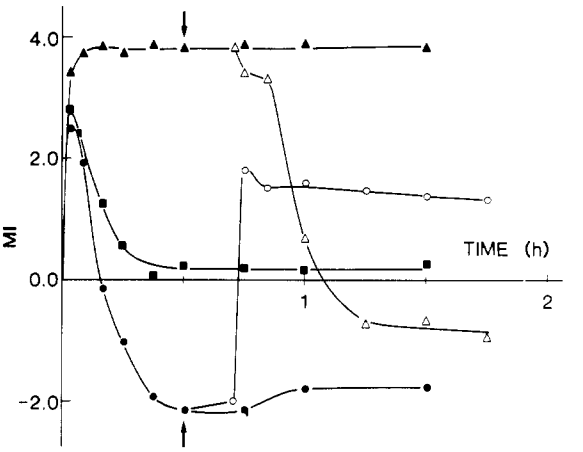

FIGURE 4: Shape reversal by DLPC and DLPS. Erythrocytes were treated with 0.2 mM DLPC (▲), 0.2 mM DLPS (●), or 0.1 mM DLPC + 0.1 mM DLPS (■). After 30 min, DLPC-induced echinocytes were washed and treated with 0.2 mM DLPS (△), and DLPS-induced stomatocytes were washed and treated with 0.2 mM DLPC (○).

Shape Reversal with Crenators. Cells were incubated with DLPS (0.20 mM) until they attained stomatocytic shape and then treated with a crenating agent, DLPC (0.20 mM). The result was a conversion of the stomatocytes to slightly echinocytic morphology (Figure 4). Conversely, DLPC-treated cells subsequently incubated with DLPS reverted to stomatocytes. Cells incubated with a cosonicated, equimolar mixture of DLPS and DLPC (0.10 mM/0.10 mM) showed an initial crenation followed by a rapid reversion to discoid shape within 20 min (closed squares, Figure 4).

Cholesterol and Lipid Extraction by Phosphatidylserine Vesicles. Supernatants from PS vesicle–erythrocyte incubations were analyzed for cholesterol and lipid. The extent of morphological change (MI) for DLPS, DMPS, DOPS, and brain PS at 0.25 mM was −1.9, −1.4, −0.8, and 0.0, respectively, after a 60-min incubation. The corresponding depletion of cell cholesterol was 7.0%, 3.4%, 2.6%, and 2.4%, respectively. Thin-layer chromatographic separation of supernatant extracts revealed the presence of PS, cholesterol, a small amount of lyso-PS, and amounts of PE and PC barely detectable by iodine staining. Supernatant lipid extracts from cells incubated 2 h with 5 mM DOPS were separated by TLC and assayed for phosphate, but any PC or PE present was below the detection limit of the assay (<1% of the total cell phospholipid).

Nontransferable Vesicle Lipid Marker. Erythrocytes were incubated with a cosonicated mixture of DMPS (0.5 mM) or DMPC (0.5 mM) and a nontransferable lipid marker, [^{14}C]cholesteryl oleate. After 60 min of incubation, the association of [^{14}C]cholesteryl oleate with cells was identical for DMPS or DMPC vesicles; approximately 2% of the label remained associated with the cells after extensive washing with NaCl/P_i.

Metabolic Processes Affecting Phosphatidylserine-Induced Stomatocytosis. Cells were treated with a variety of agents before, during, and after PS vesicle treatment to investigate the mechanism controlling PS-induced shape changes.

Amino Acid Transporter. The presence of U-0521, an amino acid transport inhibitor, or 40 mM L-tryptophan + 40 mM L-leucine [sufficient to competitively inhibit their respective transport systems (Floud & Fahn, 1981)] had no effect on DMPS-induced cell shape changes.

Calcium and Magnesium. Erythrocytes were depleted of free intracellular Ca^{2+} and Mg^{2+} by treatment with the ionophore A23187 plus 1 mM EDTA (Reed & Lardy, 1972) and

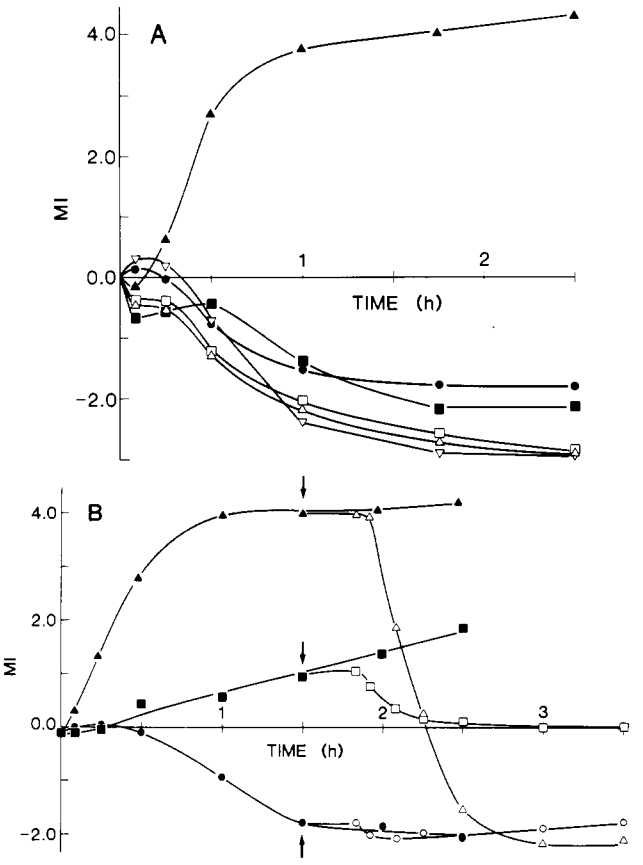

FIGURE 5: Effect of magnesium depletion and repletion on DMPS-induced shape change. (A) Shape change of erythrocytes incubated with 0.5 mM DMPS following treatment with 6.7 μM A23187 (●), 1 mM EDTA (△), 1 mM EGTA (□), 1 mM EDTA + 6.7 μM A23187 (▲), 1 mM EGTA + 6.7 μM A23187 (■), or 0.1 mM quin2/AM (▽). (B) Shape change of erythrocytes incubated with 0.5 mM DMPS in KCl/P_i following treatment with 1 mM EDTA (●) or 5 μM A23187 + 1 mM EDTA (▲) or incubated with KCl/P_i following treatment with 5 μM A23187 + 1 mM EDTA (■). The cells were washed at the time indicated by arrows, resuspended in KCl/P_i, and treated with 5 μM A23187 + 1 mM Mg^{2+} + 1 μM EGTA (open symbols).

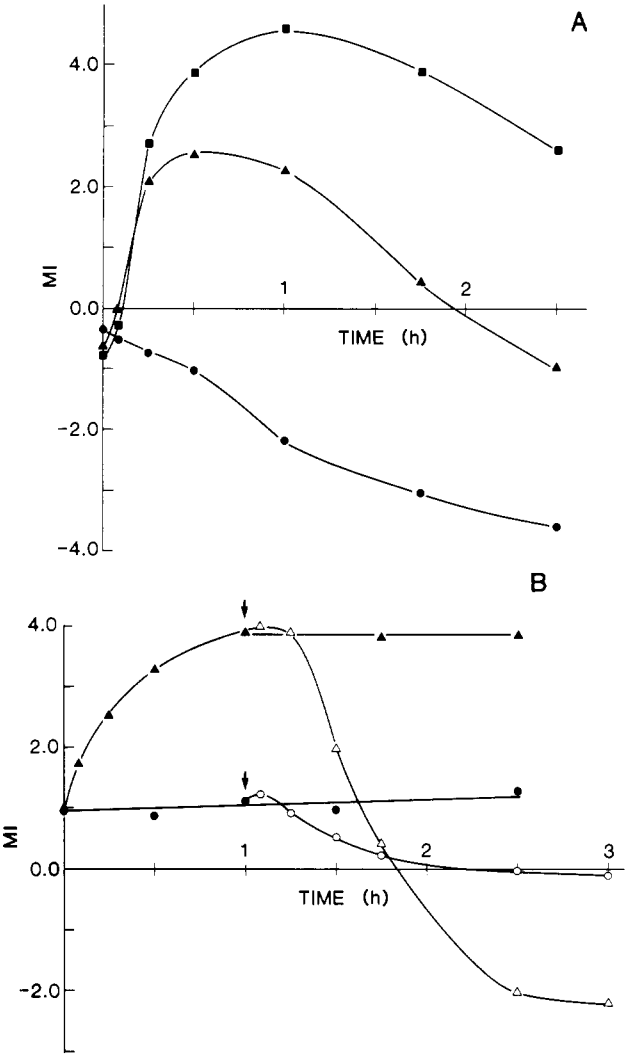

FIGURE 6: Effect of ATP depletion on DMPS-induced shape change. (A) Cells pretreated with iodoacetamide (10 mM) + inosine (6 mM) for 0 (●), 15 (▲), or 30 (■) min prior to incubation with 1 mM DMPS. (B) Cells incubated for 13.5 h without nutrients prior to treatment with 0.25 mM DMPS (▲) or NaCl/P_i (●). At the time indicated by arrows, the cells were washed twice and reincubated in buffer containing sugars (open symbols).

were depleted of free intracellular Ca^{2+} by treatment with quin2/AM (Tsien, 1981) or A23187 plus 1 mM EGTA. Control cells were treated with the ionophore or chelating agents separately. The ionophore was removed by washing with 0.1% albumin in NaCl/P_i, and cells were treated with DMPS. The shape change proceeded identically in control cells and in cells treated with quin2/AM or with the ionophore plus EGTA (Figure 5A). In contrast, cells previously treated with the ionophore plus 1 mM EDTA crenated but did not revert to stomatocytes (closed triangles, Figure 5A). EGTA or EDTA alone had no effect on the PS-induced shape change. In further experiments to determine if this apparent magnesium depletion effect is reversible and specific for Mg^{2+}, KCl/P_i buffers were used to prevent Ca^{2+}-induced K^+ loss. Cells were treated with 1 mM EDTA in KCl/P_i ± A23187, washed, and incubated with DMPS vesicles. Magnesium-depleted cells (A23187 + EDTA treated) crenated while control cells (EDTA treated) became stomatocytic (Figure 5B). Magnesium-depleted cells incubated in KCl/P_i in the absence of vesicles also crenated slowly (closed squares, Figure 5B), concurrent with a slow decrease in intracellular ATP concentration. After a 90-min incubation, cell samples were washed and reincubated in KCl/P_i containing Mg^{2+}, 1 μM EGTA, and A23187. The (A23187 + EDTA/DMPS)-induced echinocytes reverted rapidly to stomatocytes, while EDTA/DMPS stomatocytes did not change shape (open symbols, Figure 5B). Magnesium repletion also converted the slightly echinocytic control cells to normal discocytes and restored ATP concentration to normal levels. Magnesium-depleted cells also crenated when exposed to DOPS or lyso-PS but did not revert to stomatocytes unless Mg^{2+} was replenished (data not shown). The rate of reversion was similar for DOPS, lyso-PS, and DMPS.

ATP. The energy requirement of PS-induced stomatocytosis was investigated by using two methods to deplete cellular ATP: treatment with iodoacetamide plus nucleoside/sugars (Lew, 1971) and anaerobic metabolic depletion.

Erythrocytes incubated with iodoacetamide and inosine for 15 min exhibited ATP levels 60% of normal. Such cells crenated when exposed to DMPS, but the subsequent reversion to stomatocytic forms was 4-fold slower than for ATP-replete cells (Figure 6A). Depletion for 30 min under the same conditions reduced cellular ATP levels to 20% of normal; DMPS crenated these more extensively depleted cells to a greater extent, and their reversion to stomatocytes was slowed severely. ATP levels did not recover during the course of DMPS incubation.

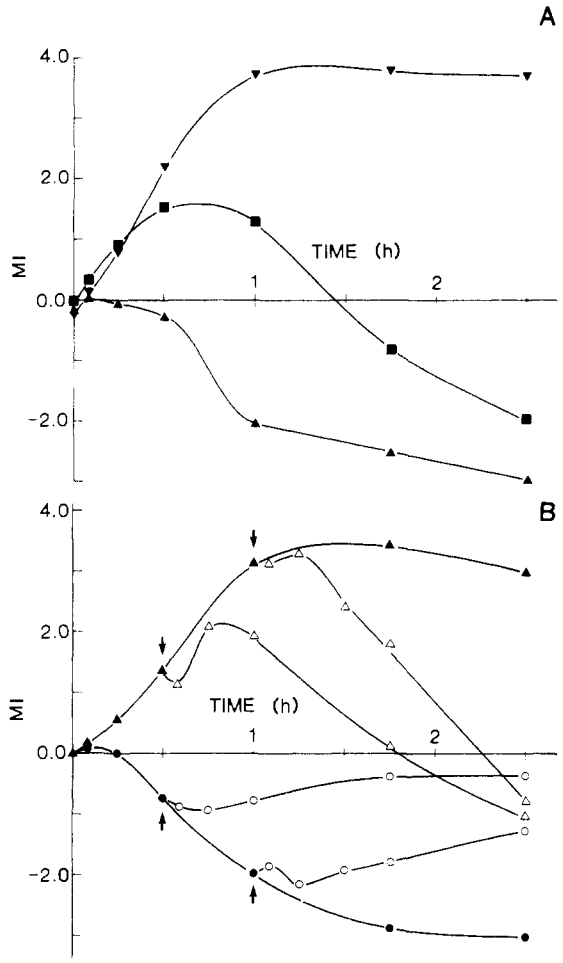

FIGURE 7: Effect of diamide treatment on DMPS-induced shape change. (A) Cells pretreated with 0.2 (▲), 1.0 (■), or 5.0 mM (▼) diamide for 1 h prior to incubation with 0.5 mM DMPS. (B) Cells pretreated with (▲) or without (●) 5 mM diamide prior to incubation with 0.5 mM DMPS. At the times indicated by arrows, cells were washed twice and reincubated in buffer containing 10 mM dithiothreitol (△) or 5 mM diamide (○).

Erythrocytes incubated under anaerobic conditions in the absence of nutrients deplete their ATP after 15–20 h and crenate after 25–30 h (Nakao et al., 1960; Ferrell & Huestis, 1984). Erythrocytes depleted in this fashion for 13.5 h (ATP levels 13% of normal) and then treated with DMPS became echinocytic rapidly and did not revert to discocytes or stomatocytes (Figure 6B). Control (closed circles, Figure 6B) cells showed only slight additional crenation during this time span. When reincubated in $NaCl/P_i$ plus sugars, ATP levels recovered, and control cells reverted to discocytes while vesicle-treated cells rapidly became stomatocytic (open symbols, Figure 6B).

Protein Sulfhydryl Redox State. Erythrocytes treated with increasing concentrations of diamide (0–5 mM) followed by DMPS exhibited increased echinocytosis and delayed reversion to stomatocytes (Figure 7A). Subsequent incubation of diamide-treated, DMPS-induced echinocytes with the sulfhydryl reducing agent dithiothreitol (10 mM) induced rapid stomatocytosis (Figure 7B). Dithiothreitol had no effect on DMPS-induced shape changes in cells not exposed to diamide. Erythrocytes treated with diamide during the course of DMPS incubation stopped changing shape, showing slight reversion toward discoid forms (open circles, Figure 7B).

Treatment after Vesicle Incubations. PS-induced stomatocytes treated with A23187 + EDTA or EGTA, iodoacetamide + inosine, or dithiothreitol did not change shape further on the time scale of these experiments.

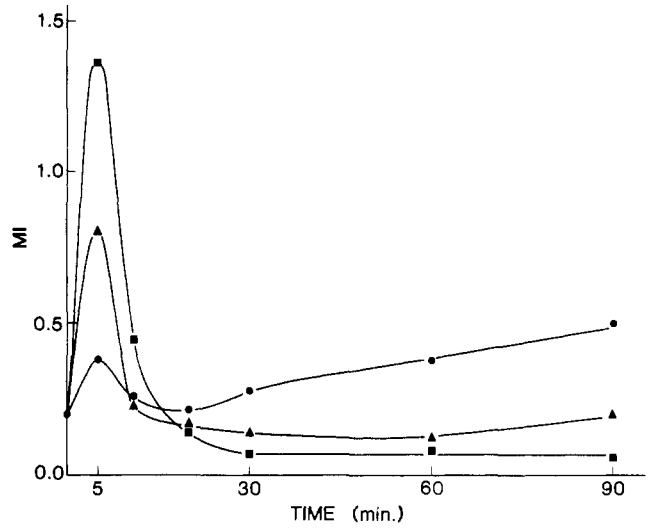

FIGURE 8: Time course of DLPS-induced platelet shape changes. Human platelets were incubated with 5 (●), 10 (▲), or 25 μM (■) DLPS and morphology indexed (MI) as described under Experimental Procedures.

Phosphatidylethanolamine. Cells treated with A23187 + EDTA, iodoacetamide + inosine, or diamide became echinocytic when exposed to DLPE but did not revert to discocytes or echinocytes (data not shown).

Phosphatidylserine Treatment of Human Platelets. Human platelets incubated with 5 μM DLPS became slightly spiculate (Figure 8). Higher concentrations (10 and 25 μM) of DLPS induced transient severe spiculation followed by recovery to a rounded and occasionally indented shape.

Discussion

The bilayer balance hypothesis provides a unified rationale for the morphological effects that amphipathic compounds exert on human erythrocytes. Preferential intercalation of such molecules into either monolayer of the cell plasma membrane disrupts its planarity, inducing the buckling characteristic of echinocytic and stomatocytic forms. The quantity of incorporated amphipath needed to produce such changes is small; calculations based on molecular dimensions of phospholipids predict that differential expansion or contraction of one lipid monolayer by 1–2% of its area is sufficient to produce the observed abnormal morphologies (Ferrell et al., 1985). This value is quantitatively consistent with spectroscopic and radiochemical studies of amphipath binding to crenated cells (Lange & Slayton, 1982; Ferrell et al., 1985). Quantitation of membrane binding of stomatocytic agents is more controversial. Some workers (Conrad & Singer, 1979; Schrier & Junga, 1981) have found that commonly studied species such as chlorpromazine partition significantly or exclusively into the cytosol, while others (Lieber et al., 1984; Pjura et al., 1984) report that the same compounds show strong preferential partitioning into lipid phases. None of these studies, however, reveals the intrabilayer distribution of the bound amphipaths, so quantitation of preferential monolayer expansion is not possible. However, the close correlation between amphipath binding and crenation has afforded an indirect way of monitoring such binding by observing changes in cell shape (Deuticke, 1968; Mohandas & Feo, 1975; Fuji et al., 1979; Lange, & Slayton, 1982; Fuji & Tamura, 1983; Ferrell et al., 1985). This approach is useful because in order for an amphipath to alter cell morphology, it must actually insert into a lipid monolayer. Thus, artifacts attendant to vesicle ad-

herence to cell surfaces and other nonnative associations can be avoided. Further, morphology provides a continuous monitor of lipid uptake and translocation.

In this study, cell morphology changes have been used to examine the association of phosphatidylserines with red cells. Other workers have shown that spin-labeled PS analogues and serine lysolipids associate transiently with the cell surface and then, on a time scale consistent with transbilayer translocation or "flip-flop", become inaccessible to reducing agents or extraction. The present findings show that DLPS, a relatively hydrophilic phospholipid, induces a rapid echinocytosis in red cells, followed by a slower reversion to discocytic and eventually stomatocytic morphology (Figure 2A). The degree of both crenation and subsequent cupping is dose dependent and roughly symmetrical; the effects are detectable with 10 μM DLPS, while maximal responses are seen in cells exposed to 1 mM exogenous lipid. These morphological effects are consistent with uptake of the foreign lipid into the cell outer leaflet, followed by slower transbilayer translocation and eventual preferential expansion of the membrane inner monolayer.

Red cells exposed to less hydrophilic serine phospholipids respond somewhat differently. DMPS has morphological effects similar to DLPS, but only at 10-fold higher concentrations. Cells incubated with 1.0 mM DMPS or DOPS show little or no initial crenation but eventually become stomatocytic (Figure 2B,C). The DMPS effect appears on a time scale similar to DLPS reversion ($t_{1/2}$ = 15–45 min), while DOPS produces stomatocytosis only after 1–3 h of incubation (Figure 2C). Bovine brain PS (acyl chain composition 18:0, 18:1) has little effect on cell shape in these time and concentration ranges, though higher (10 mM) concentrations of this lipid produce slight stomatocysis after several hours of incubation (Figure 2D).

PS-induced cell shape changes could arise by several mechanisms, among them cholesterol depletion, vesicle–cell membrane fusion, and transfer of foreign lipid to the cell by a nonfusion process such as monomer transfer through the aqueous phase. Depletion of cell cholesterol occurs when cells are incubated with vesicles composed of a variety of hydrophobic lipids (DOPC, DPPC, or egg PC). Such cells exhibit slight cupping after 15 h, coincident with loss of more than 30% of their cholesterol (Chailley et al., 1981; Lange & Slayton, 1982). The slow and limited cupping of cells incubated with brain PS is comparable to their response to DPPC vesicles and thus is consistent with cholesterol depletion. However, these effects do not proceed beyond MI's of −1 to −1.5, while cells exposed to relatively hydrophilic serine phospholipids (DLPS and DMPS) exhibit much more rapid and severe stomatocytosis. There is no evidence that DLPS or DMPS extracts cell cholesterol more rapidly or extensively than brain PS or DPPC. Moreover, equimolar mixtures of DLPS and DLPC have no long-term morphological effects (Figure 4). It is likely that some process other than cholesterol extraction is responsible for the striking morphological effects of the aminophospholipids.

It is possible that vesicle–cell fusion might produce the morphological effects seen with DLPS vesicles. The small diameter of sonicated vesicles imposes a stoichiometric imbalance between the bilayers, with 70% of the phospholipid residing in the outer monolayer (Laggner et al., 1979). If such a species fused with a cell, the preponderance of foreign lipid would appear initially in the membrane outer monolayer, producing the observed echinocytosis. The ensuing reversion to discoid and stomatocytic morphologies could then reflect slow translocation of excess lipid to the membrane inner monolayer. However, if this mechanism were operant, DLPS and DOPS would be expected to behave similarly. The rate of vesicle fusion is dependent on the lipid phase state (Papahadjopoulos et al., 1977; Düzgüneş et al., 1984) but is not otherwise affected by acyl chain composition. DLPS and DOPS are at least 15 °C above their respective gel to liquid-crystalline phase transitions under the conditions of these experiments and would be expected to undergo fusion at similar rates, yet DOPS does not produce echinocytosis at any concentration studied. Further, fusion of serine phospholipid membranes is generally a calcium-dependent process, but the cell responses to DLPS and DMPS vesicles proceed identically in the presence or absence of 1 mM EGTA. Finally, cells incubated with DMPS vesicles containing [^{14}C]cholesteryl oleate, a highly hydrophobic lipid which shows no detectable transfer between membranes through the aqueous phase, bound no more radiolabel than cells treated with DMPC/[^{14}C]cholesteryl oleate vesicles.

A third mechanism that could account for the morphological effects of PS vesicles is insertion of foreign lipid monomers into the cell membrane. The relative hydrophobicity of DLPS, DMPS, and DOPS and their differential effects on cell shape are consistent with transfer of lipid monomers through a polar medium. The relatively soluble DLPS should partition significantly into polar phases and incorporate into the cell membrane rapidly relative to the time required for transmembrane translocation. The result would be echinocytosis, followed by reversion to stomatocytosis as translocation proceeds. More hydrophobic lipids, DMPS and DOPS, might be expected to transfer through a polar phase more slowly. The stomatocytosis produced by exposure to these lipids is consistent with cell lipid uptake that is slow relative to transbilayer translocation. Brain PS, even more hydrophobic, produces no morphology change other than that attributable to cholesterol depletion. If the observed morphology changes are due to uptake (and subsequent translocation) of vesicle lipid, such changes should be proportional to the amount of bound lipid. Preliminary experiments employing [^{14}C]-DOPS-labeled DOPS vesicles (labeled additionally with the nontransferable lipid marker [^{3}H]cholesteryl oleate to permit correction for adherent vesicles) indicate that increasing stomatocytosis correlates with increasing bound [^{14}C]DOPS.

A monomer transfer process would account for the effects seen when PS vesicles are removed from cells at various morphological stages. Cells exposed to DLPS and then washed proceed to a final severely cupped state, irrespective of their morphology when the exogenous vesicles were removed (Figure 3A). Cells treated with DMPS under the same conditions stop changing shape when the exogenous lipid is removed (Figure 3B). At much higher concentrations of DMPS vesicles, the cells crenate before becoming stomatocytic, and on removal of exogenous vesicles revert rapidly to severely stomatocytic forms (Figure 3C). These observations suggest that under conditions of rapid foreign lipid uptake (as evidenced by crenation), cells will proceed to a severely cupped shape even in the absence of additional lipid sources. Where lipid transfer to cells is slow relative to transbilayer translocation, exogenous lipid sources must be present continuously to produce maximal cupping.

The stomatocytic effects of PS vesicles contrast sharply with the morphological effects of hydrophilic phosphatidylcholines. Red cells exposed to DLPC or DMPC crenate rapidly and remain echinocytic for several hours before showing signs of reversion (Fuji & Tamura, 1983). Equimolar mixtures of

DLPC and DLPS have no morphological effect on red cells, while DLPC can reverse DLPS-induced cupping and vice versa (Figure 4). Thus, incorporated foreign PC appears to remain in the cell outer monolayer while incorporated foreign PS (and PE, see Figure 2) appears to translocate to the inner monolayer.

Direct demonstration of the transbilayer distribution of the newly incorporated PS is difficult. Standard chemical (trinitrobenzenesulfonate) and enzymatic (phospholipase) techniques used to probe general phospholipid head-group distribution themselves alter cell morphology in ways that, in the case of phospholipases, increase the accessibility of membrane PC as well as other lipids (unpublished observations). The sensitivity of these assays is an additional problem; the observed morphology changes are generated by minute quantities of foreign lipid (Fuji & Tamura, 1983; Ferrell et al., 1985), such that hemolysis of as much as 1% of the cell population presents an unacceptable background. Additionally, the foreign PS need not be kinetically trapped in the inner monolayer to produce the observed morphology. If the lipid is capable of flipping, even transiently, to the outer monolayer, it will appear accessible [as to macrophages (Tanaka & Schroit, 1983)] even if its equilibrium distribution favors the inner monolayer. The slow reversion of diamide-treated PS stomatocytes toward discoid forms (Figure 7B) might reflect such flipping, reversing PS-induced stomatocytosis when the active translocation mechanism is compromised. Finally, while the present findings do not demonstrate that the foreign PS per se is the translocated species, the report (Seigneuret & Devaux, 1984) that spin-labeled PS analogues are translocated selectively would support a head-group-specific mechanism. Such selectivity would act to preserve the normal asymmetric lipid distribution between the cell monolayers and may thus provide information on the mechanism whereby that distribution is maintained. Monitoring cell morphology changes provides a sensitive and powerful way to examine the biochemistry of this translocation mechanism.

Magnesium and ATP Dependence. The present results indicate that PS-induced stomatocytosis is ATP dependent, as reported for the translocation of spin-labeled PS (Seigneuret & Devaux, 1984). Erythrocytes depleted of intracellular ATP by incubation with iodoacetamide + nucleosides/sugars show dose-dependent alterations in DMPS-induced morphology changes (Figure 6A). Cells with ATP levels reduced by 58–83% show an increase in the extent and duration of echinocytosis. This indicates that the first phase of PS- or PE-induced shape change, foreign lipid incorporation into the outer membrane leaflet, is not ATP dependent. This crenation is not due to metabolic depletion, since iodoacetamide-treated control cells do not crenate significantly on this time scale. The second phase of shape change is slowed in ATP-depleted cells and almost stopped in severely depleted cells. PS and PE translocation, therefore, appears to require intracellular ATP. However, as iodoacetamide also alkylates erythrocyte proteins and depletes intracellular glutathione, this effect might be due to other events in addition to ATP depletion.

Metabolic depletion without extensive cell oxidation can be accomplished by incubating cells without nutrients under humidified argon. Depletion under these conditions for 13.5 h removes most (87%) intracellular ATP and only partially depletes (20%) cell glutathione. Subsequent treatment with DMPS induces rapid echinocytosis with little or no recovery after 2.5 h, consistent with ATP-independent lipid incorporation and diminished ATP-dependent translocation. Restoration of ATP levels by nutrient supplementation produces rapid reversion to stomatocytic forms, consistent with recovery of PS translocation capacity.

These shape changes also depend on intracellular divalent cations; cell suspended in EDTA plus the ionophore A23187 crenate upon exposure to DMPS but do not revert to stomatocytes (closed triangles, Figure 5A). The cation requirement probably is for Mg^{2+}; when A23187 + EDTA is replaced by A23187 + EGTA in the foregoing experiment, DMPS-treated cells proceed to stomatocytes as usual (closed squares, Figure 5A). The calcium-specific intracellular chelator quin2/AM also has no effect on DMPS-induced stomatocytosis. The effects of Mg^{2+} depletion are reversible; when (A23187 + EDTA/DMPS)-treated echinocytes are exposed to fresh buffer containing Mg^{2+} (1 mM), A23187, and EGTA (1 μM), they revert rapidly to stomatocytes (Figure 5B). Similar results are found with DOPS and lyso-PS (data not shown).

Acyl Chain Dependence. For both PC and PS, vesicle to cell transfer rates depend strongly on lipid acyl chain composition (Figure 2; Fuji & Tamura, 1983; Ferrell et al., 1985). PC flip-flop rates in erythrocytes increase with increasing acyl chain unsaturation (Van Meer & Op den Kamp, 1982), and the reversal of saturated PC- and lyso-PC-induced crenation is more rapid for lipids with shorter acyl chains (Fuji & Tamura, 1983). In contrast, the stomatocytic phase of the PS-induced shape change proceeds at a rate independent of PS acyl chain composition. ATP or Mg^{2+} repletion of DMPS- (Figures 5B and 6B) or DOPS-induced echinocytes causes reversion to stomatocytes on the same time scale, similar to DLPS stomatocytosis of normal cells (Figure 2A). Moreover, lyso-PC flip-flop is not ATP dependent (Mohandas et al., 1982; Bergmann et al., 1984b). Thus, the stomatocytosis apparently generated by PS translocation involves a mechanism distinct from PC flip-flop.

Effect of Sulfhydryl Group Oxidizing Agents. The phospholipid head-group asymmetry of human red cell membranes is thought to depend in part on the oxidative state of cell proteins; oxidative cross-linking of cells with diamide results in partial loss of PS asymmetry (Haest & Deuticke, 1976). Cytoskeletal proteins, including spectrin, are extensively cross-linked by diamide treatment and have been implicated as binding sites for PS (Sweet & Zull, 1970; Haest et al., 1978; Mombers et al., 1979), maintaining PS asymmetry by trapping this lipid in the inner leaflet. Diamide cross-linking also increases the translocation of PC (Franck et al., 1982), lyso-PS, and lyso-PC (Bergmann et al., 1984a; Mohandas et al., 1982), possibly by increasing access of these lipids to transmembrane reorientation sites. These sites may be equivalent to the aqueous pores formed in erythrocyte membranes by diamide treatment (Deuticke et al., 1983). In the present work, cells treated with 5 mM diamide, washed, and exposed to DMPS vesicles crenate but do not revert to stomatocytes (Figure 7A). Reduction of these echinocytes with dithiothreitol results in reversion to cupped forms (Figure 7B). Diamide alone has little or no effect on the morphology of stomatocytes, discocytes, or PC-induced echinocytes on the time scale of these experiments. The sulfhydryl alkylating agent *N*-ethylmaleimide also prevents PS-induced stomatocytosis (unpublished observations); thus, sulfhydryl modification rather than cross-linking per se appears responsible for these effects.

The dependence of PS-induced stomatocytosis on Mg^{2+}, ATP, and the sulfhydryl state of erythrocyte proteins is unique to the serine phospholipids; other cup formers, such as chlorpromazine (Deuticke, 1968), induce stomatocytosis in cells pretreated with diamide, iodoacetamide + nucleosides/sugars, or A23187 + EDTA (unpublished observations).

Amino Acid Transport Inhibition. The human erythrocyte possesses an amino acid transporter (Young & Ellory, 1977; Rosenberg et al., 1980) which could transport PS as an amino acid analogue. Although negatively charged amino acids have negligible transport rates into human erythrocytes, amino acids with lipophilic side chains are transported more rapidly (Young & Ellory, 1977). Inhibition of the human erythrocyte amino acid transporter with 40 mM tryptophan + 40 mM leucine or with U-0521 has no net effect on the PS-induced shape change, ruling out involvement of the amino acid transport system in PS translocation. In addition, DLPE is not an amino acid analogue, yet this work indicates that it is translocated by a mechanism similar to PS.

Lyso-PS-Induced Shape Changes. The morphological responses observed in these experiments differ in degree from those reported for cells treated with lyso-PS and spin-labeled PS analogues (Bergmann et al., 1984b; Seigneuret & Devaux, 1984). As shown in Figure 2E, cells exposed to lyso-PS suspensions crenate rapidly and then return to discoid shape but show little stomatocytosis. Similar results have been reported for the spin-labeled PS 1-palmitoyl-2-(4-doxylpentanoyl)-PS, which resembles lyso-PS in having an abbreviated and polar moiety in the position normally occupied by the β-acyl chain (Seigneuret & Devaux, 1984). The reason for this difference is unclear; the fully substituted phospholipids might be expected to occupy more space in the monolayer and have greater influence per molecule, but such an effect should be apparent during the crenation phase as well as stomatocytosis. Cells crenated with lyso-PS to an extent apparently identical with DLPS crenation stop changing shape at MI = −0.5, while DLPS-treated cells continue to MI = −3.5 to −4.0 (Figure 2A,E). This difference cannot be attributed to the fully saturated acyl chains in DLPS; DOPS (18:1, 18:1) also induces stage −4 stomatocytosis. The metabolic requirements for lyso-PS translocation are similar to those for diacyl-PS's. Diamide treatment and Mg^{2+} depletion prevent the reversion of lyso-PS-treated cells to discocytes (data not shown). Subsequent addition of Mg^{2+} to Mg^{2+}-depleted cells immediately restores the lyso-PS translocating capacity. Phospholipase experiments in progress will address the question of whether lyso-PS is translocated less completely than fully acylated PS.

PS-Induced Platelet Shape Changes. Platelets are circulating fragments with an asymmetric arrangement of membrane lipids similar to red cells (Chap et al., 1977). In addition, platelets have been shown to change shape when treated with inner or outer membrane monolayer intercalators in a fashion analogous to erythrocytes (Kobayashi et al., 1984; J. E. Ferrell, Jr., K. T. Mitchell, and W. H. Huestis, unpublished observations). When treated with crenators, they produce long filopodia, and when treated with inner monolayer intercalators, they become rounded and indented. Inner and outer monolayer intercalators also reverse the morphological effects of one another in platelets as well as red cells.

We investigated the generality of PS-induced cell shape changes by treating human platelets with DLPS. As with erythrocytes, platelets show a biphasic shape change. When treated with high concentrations of DLPS, the cells become transiently spiculate and subsequently reverse to rounded, indented shapes. Lower concentrations cause less spiculation although even at the lowest concentration some spiculation occurs. These results [and others; see Bevers et al. (1983)] indicate that platelets may have a mechanism for maintaining membrane phospholipid asymmetry similar to erythrocytes.

Conclusions

These studies have employed cell shape changes to monitor the association of exogenous phosphatidylserines with human erythrocytes. The results are consistent with earlier studies using lyso-PS and spin-labeled PS; the foreign lipid appears to be incorporated into the membrane outer monolayer and then translocated to the inner monolayer with consequent cupping of the cells. The process is dependent upon Mg^{2+}, ATP, and the sulfhydryl group status of cell proteins. As the second and third of these factors influence transbilayer distribution in normal cells, the observed translocation events may bear on the mechanism of maintenance of membrane phospholipid asymmetry.

Acknowledgments

We thank Kathleen T. Mitchell for preparing the human platelets and Dr. James E. Ferrell, Jr., for assistance in platelet morphological indexing.

Registry No. 5′-ATP, 56-65-5; DLPS, 2954-46-3; DMPS, 64023-32-1; DOPS, 6811-55-8; DLPE, 42436-56-6; DLPC, 18285-71-7; Mg, 7439-95-4; cholesterol, 57-88-5.

References

Bartlet, G. R. (1959) *J. Biol. Chem. 234*, 466–468.
Beck, J. S. (1978) *J. Theor. Biol. 75*, 487–501.
Bergmann, W. L., Dressler, V., Haest, C. W. M., & Deuticke, B. (1984a) *Biochim. Biophys. Acta 769*, 390–398.
Bergmann, W. L., Dressler, V., Haest, C. W. M., & Deuticke, B. (1984b) *Biochim. Biophys. Acta 772*, 328–336.
Beutler, E. (1975) in *Red Cell Metabolism* (Beutler, E., Ed.) 2nd ed., pp 112–114, Grune & Stratton, New York.
Bevers, E. M., Comfurius, P., & Zwaal, R. F. A. (1983) *Biochim. Biophys. Acta 736*, 57–66.
Bligh, E. G., & Dyer, W. J. (1959) *Can. J. Biochem. Physiol. 37*, 911–917.
Chailley, B., Giraud, F., & Claret, M. (1981) *Biochim. Biophys. Acta 643*, 636–641.
Chap, H. J., Zwaal, R. F. A., & Van Deenen, L. L. M. (1977) *Biochim. Biophys. Acta 467*, 146–164.
Comfurius, P., & Zwaal, R. F. A. (1972) *Biochim. Biophys. Acta 448*, 36–42.
Conrad, M. J., & Singer, S. J. (1979) *Proc. Natl. Acad. Sci. U.S.A. 76*, 5202–5206.
Deuticke, B. (1968) *Biochim. Biophys. Acta 163*, 494–500.
Deuticke, B., Poser, B., Lutkemeier, P., & Haest, C. W. M. (1983) *Biochim. Biophys. Acta 731*, 196–210.
Dressler, V., Haest, C. W. M., Plasa, G., Deuticke, B., & Erusalimsky, J. D. (1984) *Biochim. Biophys. Acta 775*, 189–196.
Düzgüneş, N., Paiement, J., Freeman, K. B., Lopez, N. G., Wilschut, J., & Papahadjopoulos, D. (1984) *Biochemistry 23*, 3486–3494.
Etemadi, A.-H. (1980) *Biochim. Biophys. Acta 604*, 423–475.
Ferrell, J. E., & Huestis, W. H. (1984) *J. Cell Biol. 98*, 1992–1998.
Ferrell, J. E., Lee, K. J., & Huestis, W. H. (1985) *Biochemistry 24*, 2849–2864.
Floud, A., & Fahn, S. (1981) *Biochim. Biophys. Acta 645*, 165–169.
Franck, P. F. H., Roelofsen, B., & Op den Kamp, J. A. F. (1982) *Biochim. Biophys. Acta 687*, 105–108.
Fuji, T., & Tamura, A. (1983) *Biomed. Biochim. Acta 42*, 581–585.
Fuji, T., Sato, T., Tamura, A., Watkatsuki, M., & Kanaha, Y. (1979) *Biochem. Pharmacol. 28*, 613–620.

Haest, C. W. M., & Deuticke, B. (1976) *Biochim. Biophys. Acta 436*, 353-365.
Haest, C. W. M., Plasa, G., Kamp, D., & Deuticke, B. (1978) *Biochim. Biophys. Acta 509*, 21-32.
Kimmich, G. A., Randles, A. J., & Brand, J. S. (1975) *Anal. Biochem. 69*, 187-206.
Kobayashi, T., Okamoto, H., Yamada, J.-I., Setaka, M., & Kwan, T. (1984) *Biochim. Biophys. Acta 778*, 210-218.
Laggner, P., Gotto, A. M., & Morrisett, J. D. (1979) *Biochemistry 18*, 164-171.
Lange, Y., & Slayton, J. M. (1982) *J. Lipid Res. 23*, 1121-1127.
Lew, V. L. (1971) *Biochim. Biophys. Acta 233*, 827-830.
Lieber, M. R., Lange, Y., Weinstein, R. S., & Steck, T. L. (1984) *J. Biol. Chem. 259*, 9225-9234.
Mohandas, N., & Feo, C. (1975) *Blood Cells 1*, 375-384.
Mohandas, N., Greenquist, A. C., & Shohet, S. B. (1978) *J. Cell. Biochem. 9*, 453-458.
Mohandas, N., Wyatt, J., Mel, S. F., Rossi, M. E., & Shohet, S. B. (1982) *J. Biol. Chem. 257*, 6537-6543.
Mombers, C., Verkleij, A. J., DeGier, J., & Van Deenen, L. L. M. (1979) *Biochim. Biophys. Acta 551*, 271-281.
Nakao, M., Nakao, T., & Yamazoe, S. (1960) *Nature (London) 187*, 945-946.
Op den Kamp, J. A. F. (1979) *Annu. Rev. Biochem. 48*, 47-71.
Papahadjopoulos, D., Vail, W. J., Newton, C., Nir, S., Jacobson, K., Poste, G., & Lazo, R. (1977) *Biochim. Biophys. Acta 465*, 579-598.
Pjura, W. J., Kleinfeld, A. M., & Karnovsky, M. J. (1984) *Biochemistry 23*, 2039-2043.
Reed, P. W., & Lardy, H. A. (1972) *J. Biol. Chem. 247*, 6970-6977.
Roelofsen, B., & Zwaal, R. F. A. (1976) *Methods Membr. Biol. 7*, 147-177.
Rosenberg, R., Young, J. D., & Ellory, J. C. (1980) *Biochim. Biophys. Acta 598*, 375-384.
Schrier, S. L., & Junga, I. (1981) *Proc. Soc. Exp. Biol. Med. 168*, 159-167.
Schwartz, R. S., Chiu, D. T.-Y., & Lubin, B. (1985) *Curr. Top. Hematol. 5*, 63-112.
Seigneuret, M., & Devaux, P. F. (1984) *Proc. Natl. Acad. Sci. U.S.A. 81*, 3751-3755.
Sheetz, M. P., & Singer, S. J. (1974) *Proc. Natl. Acad. Sci. U.S.A. 71*, 4457-4461.
Sweet, C., & Zull, J. E. (1970) *Biochem. Biophys. Res. Commun. 41*, 135-141.
Tanaka, Y., & Schroit, A. J. (1983) *J. Biol. Chem. 258*, 11335-11343.
Tsien, R. Y. (1981) *Nature (London) 290*, 527-528.
Tsien, R. Y., Pozzan, T., & Rink, T. J. (1982) *J. Cell Biol. 94*, 325-334.
Van Deenen, L. L. M. (1981) *FEBS Lett. 123*, 3-15.
Van Meer, G., & Op den Kamp, J. A. F. (1982) *J. Cell. Biochem. 19*, 193-204.
Young, J. D., & Ellory, J. C. (1977) in *Membrane Transport in Red Cells* (Ellory, J. C., & Lew, V. L., Eds.) pp 301-325, Academic Press, New York.
Zlatkis, A., Zak, B., & Boyle, A. J. (1953) *J. Lab. Clin. Med. 41*, 486-492.

Reactivities of Tyrosine, Histidine, Tryptophan, and Methionine in Radical Pair Formation in Flavin Triplet Induced Protein Nuclear Magnetic Polarization

Karol A. Muszkat* and Tmima Wismontski-Knittel

Department of Structural Chemistry, The Weizmann Institute of Science, Rehovot 76100, Israel

Received September 19, 1984; Revised Manuscript Received March 7, 1985

ABSTRACT: In order to check the validity of several basic assumptions of protein photochemically induced nuclear polarization (protein photo-CIDNP), we have investigated the quenching processes of the dye triplets by the side chains of tyrosine, histidine, and tryptophan in a variety of molecular systems and environments. The quenching (H atom or electron transfer) is the generating process of the triplet electron-spin-correlated radical pair, the evolution of which gives rise to nuclear polarization. At pH 7 the quenching of 10-(carboxyethyl)flavin triplets by tyrosine and tryptophan is almost diffusion controlled. Quenching by histidine is slower. We have also investigated the slow quenching (by electron transfer) by the side chains of methionine and could show that quenching by cysteine S derivatives is negligible. Quenching by tyrosine and histidine peptides and by the tyrosines of the pancreatic trypsin inhibitor protein is slightly slower than by free side chains. Quenching is strongly viscosity controlled, to be expected of a process requiring bimolecular contact. Reactivity trends at high viscosities resemble those observed in fluid aqueous solutions. Activation energies of quenching by tyrosine, tryptophan, and histidine are similar. No difference could be detected in the mechanism of quenching by these side chains. No fast static quenching was observed that could compete with the diffusional process.

Protein photo-CIDNP[1] measurements serve as a highly specific and sensitive tool for studies of accessibility of active[1] side chains of proteins in solution. The same measurements show promise in studies of protein-protein interactions, as a

0006-2960/85/0424-5416$01.50/0